General-relativistic versus Newtonian: Geometric dragging and dynamic antidragging in stationary self-gravitating disks in the first post-Newtonian approximation

Piotr Jaranowski

Wydział Fizyki, Uniwersytet w Białymstoku, Lipowa 41, 15-424 Białystok, Poland

Patryk Mach, Edward Malec, and Michał Piróg

*Instytut Fizyki Mariana Smoluchowskiego, Uniwersytet Jagielloński,
Łojasiewicza 11, 30-348 Kraków, Poland*

We evaluate general-relativistic effects in the motion of stationary self-gravitating accretion disks around a Schwarzschild black hole, assuming the first post-Newtonian (1PN) approximation. There arises an integrability condition that leads to the emergence of two types of general-relativistic corrections to a Newtonian rotation curve. The well-known geometric dragging of frames accelerates rotation, but the hitherto unknown dynamic term, that reflects the disk structure, decelerates rotation. The net result can diminish the Newtonian angular velocity of rotation in a central disk zone, but the geometric dragging of frames dominates in the disk boundary zone. Both effects are nonlinear in nature, and they disappear in the limit of test fluids. Dust disks can only be geometrically dragged, while uniformly rotating gaseous disks are untouched at the 1PN order. General-relativistic contributions can strongly affect rotation periods in Keplerian motion for compact systems.

PACS numbers: 04.20.-q, 04.25.Nx, 04.40.Nr, 95.30.Sf

I. INTRODUCTION

Rotation curves are important characteristics of stationary accretion disks. Angular velocities can be determined from observations of astrophysical systems, and they allow for the direct determination of the central mass when disks are light and their self-gravity can be neglected [1,2]. For heavy disks the self-gravity must be included, and even in the Newtonian case one can give only a rough estimate of the central mass [3]. Additional information on the disk geometry and modeling would be required to learn more about masses of observed objects. This approach has been applied to NGC 4258, the unique AGN with a well-measured Keplerian rotation curve of the central disk [4]. A well-known feature of axially symmetric Newtonian accretion disks is that rotation curves of fluids depend only on the distance to the rotation axis and do not depend on the distance to the plane of symmetry.

The principal aim of this paper is to investigate general-relativistic corrections to Newtonian rotation curves in systems with stationary accretion disks. We take into account the self-gravity of the accretion disk and in numerical analysis specialize to the Keplerian rotation law, at the 0PN (Newtonian) level. The 1PN approximation scheme is employed, following Blanchet, Damour, and Schäfer [5].

The existing research on general-relativistic accretion disks focuses mainly on test systems in a prescribed spacetime geometry. The literature is extensive, to mention a pioneering paper by Bardeen and Wagoner [6] and an early review by Novikov and Thorne [2]. Recent reviews have been written by Karas, Hure, and Semerak [7]; Abramowicz and Fragile [8]; and Stergioulas [9]. See also numerous references therein. We should mention here the work of Fishbone and Moncrief, who studied the influence of the black hole's angular momentum on the disk structure for the stationary flow of isentropic fluid in Kerr geometry [10].

The first general-relativistic formulation of thick self-gravitating disks (around a black hole or a star) has been derived by Nishida, Lanza, and Eriguchi [11,12]. They found in particular the dragging of inertial frames due to rotating toroids for general-relativistic extensions of two types of Newtonian rotation curves: uniform angular velocity and constant specific angular momentum. Ansorg and Petroff [13] studied numerically a disk–black hole system from a different perspective, focusing on the geometry of the apparent horizon and its parametrization.

The order of this work is as follows: The relevant equations in the 1PN approximation are given in Sec. II. Section III displays final equations, under the simplifying assumption of axial symmetry. In Sec. IV, we show that the consistency of 1PN equations imposes an integrability condition. That yields a dual structure of the corrections to the Newtonian rotation curve. One of the terms can be recognized as the well-known geometric dragging of frames induced indirectly (via the backreaction effect) by the disk rotation. The other depends on the specific enthalpy, and thus it has a dynamic, material character. In Sec. V we prove that the dynamic term decelerates rotation, while the geometric effect increases the angular velocity.

A scaling symmetry of Euler equations allows one to find a simple scaling law for the 1PN angular velocity correction and for its ratio to the Newtonian angular velocity. The post-Newtonian corrections are analyzed for fluids and dust, and for different rotation curves.

It is notable that rigid rotation is untouched by 1PN corrections, while dust disks are influenced only by the geometric drag. Section VI is dedicated to the description of the numerical approach to the problem. The obtained results are discussed in Sec. VII. It appears—in agreement with analytic results—that the two effects, geometric and dynamic, work against each other and that absolute values of their extrema are comparable. As a consequence, the net general-relativistic 1PN effect is weakest (can vanish), paradoxically, in a central disk zone where the two component parts taken separately are strongest. The dynamic component vanishes at the disk boundary; thus the dragging of frames dominates in the disk boundary zone. The important feature seen in the 1PN approximation, that may have observational consequences, is that the rotation curve depends on the height above the plane of disk symmetry. Finally, we summarize obtained results and point out open questions.

II. EQUATIONS

Einstein equations, with the signature $(-, +, +, +)$, read

$$R_{\mu\nu} - g_{\mu\nu}\frac{R}{2} = 8\pi\frac{G}{c^4}T_{\mu\nu}, \qquad (2.1)$$

where $T_{\mu\nu}$ is the stress-momentum tensor. The *stationary* metric is given in the form suitable for the 1PN approximation, in Cartesian coordinates $x = x^1$, $y = x^2$, $z = x^3$, $x^0 = ct$, by

$$
\begin{aligned}
\mathrm{d}s^2 &= \left(-1 - 2\frac{U(x,y,z)}{c^2} - 2\frac{(U(x,y,z))^2}{c^4}\right)(\mathrm{d}x^0)^2 \\
&\quad - 2\frac{A_i(x,y,z)}{c^3}\mathrm{d}x^i\mathrm{d}x^0 \\
&\quad + \left(1 - 2\frac{U(x,y,z)}{c^2}\right)(\mathrm{d}x^2 + \mathrm{d}y^2 + \mathrm{d}z^2). \quad (2.2)
\end{aligned}
$$

In the remainder of this section we use Cartesian coordinates. We employ the stress-momentum tensor of the form

$$T^{\alpha\beta} = T_{\mathrm{BH}}^{\alpha\beta} + T_{\mathrm{D}}^{\alpha\beta}, \qquad (2.3)$$

where $T_{\mathrm{BH}}^{\alpha\beta}$ describes the point particle (which models the central black hole) at rest located at the origin of the coordinate system and $T_{\mathrm{D}}^{\alpha\beta}$ is the stress-momentum tensor

of the disk matter. The tensor $T_{\mathrm{BH}}^{\alpha\beta}$ describing a single point particle is proportional to the Dirac delta distribution,

$$T_{\mathrm{BH}}^{\alpha\beta} = \frac{M_{\mathrm{c}}c^2}{\sqrt{g}}\frac{u_{\mathrm{BH}}^{\alpha}u_{\mathrm{BH}}^{\beta}}{u_{\mathrm{BH}}^0}\delta(\mathbf{x} - \mathbf{z}_{\mathrm{BH}}(t)), \qquad (2.4)$$

where M_{c} is the mass parameter of the point particle, $g := -\det(g_{\mu\nu})$, and $u_{\mathrm{BH}}^{\alpha} := \mathrm{d}z_{\mathrm{BH}}^{\alpha}/(c\mathrm{d}\tau_{\mathrm{BH}})$ is the 4-velocity along the particle's world line parametrized by the proper time τ_{BH}. We assume that the point particle is located at rest at the origin of the coordinate system, therefore $\mathbf{z}_{\mathrm{BH}}(t) \equiv \mathbf{0}$; then $T_{\mathrm{BH}}^{\alpha\beta}$ simplifies to

$$T_{\mathrm{BH}}^{00} = \frac{M_{\mathrm{c}}c^2}{\sqrt{g}}(u_{\mathrm{BH}}^0)^2\delta(\mathbf{x}), \qquad T_{\mathrm{BH}}^{0i} = T_{\mathrm{BH}}^{ij} = 0. \quad (2.5)$$

The disk is made of perfect fluid with a stress-momentum tensor

$$T_{\mathrm{D}}^{\alpha\beta} = \rho(c^2 + h)u^{\alpha}u^{\beta} + pg^{\alpha\beta}, \qquad (2.6)$$

where ρ is the baryonic rest-mass density, h is the specific enthalpy, and p is the pressure. The 4-velocity $u^{\alpha} := \mathrm{d}x^{\mu}/(c\mathrm{d}\tau)$ along the world line of fluid particles is normalized (τ is their proper time), $g_{\alpha\beta}u^{\alpha}u^{\beta} = -1$.

The proper specific enthalpy h is related with the proper relativistic energy density e through the relation

$$h = \frac{e + p}{\rho} - c^2. \qquad (2.7)$$

We assume the polytropic equation of state

$$e(\rho, S) = \rho c^2 + \frac{K(S)}{\gamma - 1}\rho^{\gamma}, \qquad (2.8)$$

where S is the specific entropy of fluid. Then the following relations hold:

$$p(\rho, S) = \rho\left(\frac{\partial e}{\partial \rho}\right)_S - e = K(S)\rho^{\gamma}, \qquad (2.9)$$

$$h(\rho, S) = K(S)\frac{\gamma}{\gamma - 1}\rho^{\gamma-1}. \qquad (2.10)$$

In this paper we assume that the entropy is constant.

The 1PN-accurate stationary relativistic Euler equation can be derived directly from the conservation law, $\nabla_{\alpha}T^{\alpha\beta} = 0$, and the continuity of the baryonic current, $\nabla_{\alpha}(\rho u^{\alpha}) = 0$. Alternatively, one can employ Eq. (2.18) in Ref. [5]. The result reads

$$
\begin{aligned}
\partial_j(\rho v^i v^j + c^{-2}\rho v^j(-A_i + v^i(h - 6U + \mathbf{v}^2)) &+ (1 - 2c^{-2}U)p\delta_i^j) = -(\rho + M_{\mathrm{c}}(1 + c^{-2}U)\delta(\mathbf{x}) \\
&+ c^{-2}(2p + \rho(h - 2U + 2\mathbf{v}^2)))\partial_i U - c^{-2}\rho v^j \partial_i A_j, \quad (2.11)
\end{aligned}
$$

where $v^i := dx^i/dt$ is the coordinate velocity of the fluid particle and $\mathbf{v}^2 := \delta_{ij}v^iv^j$. The scalar potential U is the solution of the following 1PN-accurate equation:

$$\Delta U = 4\pi G(\rho + M_c(1 + c^{-2}U)\delta(\mathbf{x})$$
$$+ c^{-2}(2p + \rho(h - 2U + 2\mathbf{v}^2))), \quad (2.12)$$

and the vector potential A_i fulfills the equation

$$\Delta A_i = -16\pi G\rho v_i, \quad (2.13)$$

where Δ is the flat Laplacian. Asymptotically we have $|\mathbf{A}| \propto 4J/R$, where J is the total angular momentum of the configuration and $R := \sqrt{x^2 + y^2 + z^2}$ is the coordinate cylindrical radius. In the case of stationary configurations the 1PN-accurate continuity equation for the perfect fluid with the stress-momentum tensor (2.6) reads

$$0 = \partial_i(\sqrt{g}u^0\rho v^i)$$
$$= \partial_i\left(\rho v^i + c^{-2}\rho v^i\left(\frac{1}{2}\mathbf{v}^2 - 3U\right)\right) + \mathcal{O}(c^{-4}). \quad (2.14)$$

III. AXIALLY SYMMETRIC DISKS

Let us now assume axial and equatorial symmetry. We shall replace the Cartesian coordinates (x, y, z) with cylindrical ones (r, ϕ, z), where $x = r\cos\phi$, $y = r\sin\phi$. Axial symmetry means that the only nonzero cylindrical components of the 3-vector field $\mathbf{v}$ and the 3-covector field $\mathbf{A}$ are the azimuthal components v^ϕ and A_ϕ, respectively: $\mathbf{A} = A_\phi d\phi$ and $\mathbf{v} = v^\phi\partial_\phi$. These two components and the scalar quantities ρ, p, h, U all do not depend on ϕ.

We split different quantities (ρ, p, h, U, and v^i) into their Newtonian (denoted by subscript "0") and 1PN (denoted by subscript "1") parts. E.g., for the baryonic rest-mass density ρ and the fluid velocity v^i, this splitting reads

$$\rho = \rho_0 + c^{-2}\rho_1, \quad (3.1a)$$

$$v^\phi = v_0^\phi + c^{-2}v_1^\phi. \quad (3.1b)$$

Notice that, up to 1PN order,

$$\frac{1}{\rho}\partial_i p = \partial_i h_0 + c^{-2}\partial_i h_1 + \mathcal{O}(c^{-4}), \quad (3.2)$$

where the 1PN correction h_1 to the specific enthalpy can be written as

$$h_1 = (\gamma - 1)h_0\frac{\rho_1}{\rho_0}. \quad (3.3)$$

One can easily derive from Eq. (3.2) useful relations connecting gradients of pressure and specific enthalpy at the Newtonian and 1PN levels:

$$\partial_i p_0 = \rho_0\partial_i h_0, \qquad \partial_i p_1 = \rho_0\partial_i h_1 + \rho_1\partial_i h_0. \quad (3.4)$$

Making use of the splitting of quantities into Newtonian and 1PN parts introduced above, one can extract from Eq. (2.11) the Newtonian- and 1PN-level Euler equations. The Newtonian equations read

$$\nabla_j(\rho_0 v_0^i v_0^j) + \partial_i p_0 = -\rho_0\partial_i U_0 + \partial_i U_0 M_c\delta(\mathbf{x}). \quad (3.5)$$

The 1PN Euler equations take the form

$$\nabla_j(\rho_0(v_0^i v_1^j + v_1^i v_0^j) + \rho_1 v_0^i v_0^j + \rho_0 v_0^j(-A_i + v_0^i(h_0 - 6U_0 + r^2(v_0^\phi)^2)) + (p_1 - 2p_0 U_0)\delta_i^j)$$
$$= -(\partial_i U_1 + U_0\partial_i U_0)M_c\delta(\mathbf{x}) - (\rho_1 + 2p_0 + \rho_0(h_0 - 2U_0 + 2r^2(v_0^\phi)^2))\partial_i U_0 - \rho_0\partial_i U_1 - \rho_0 v_0^j\partial_i A_j. \quad (3.6)$$

The splitting of the potential U into its Newtonian U_0 and 1PN U_1 parts reads

$$U = U_0 + c^{-2}U_1. \quad (3.7)$$

The determination of U_0 needs only material fluid quantities of zeroth order, while U_1 requires also the 1PN density correction ρ_1:

$$\Delta U_0 = 4\pi G(M_c\delta(\mathbf{x}) + \rho_0), \quad (3.8a)$$

$$\Delta U_1 = 4\pi G(M_c U_0\delta(\mathbf{x}) + \rho_1 + 2p_0$$
$$+ \rho_0(h_0 - 2U_0 + 2r^2(v_0^\phi)^2)). \quad (3.8b)$$

The disk mass at the Newtonian level is equal to $M_D = \int_V d^3x\rho_0$, and the total mass of the system is

$M_c + M_D$. The 1PN mass correction M_{1PN} can be read off from the asymptotic expansion of the correction potential U_1. It is given by

$$M_{1PN} = \int_V d^3x 4\pi G(M_c U_0\delta(\mathbf{x}) + \rho_1 + 2p_0$$
$$+ \rho_0(h_0 - 2U_0 + 2r^2(v_0^\phi)^2)).$$

The right-hand sides of Eqs. (3.5), (3.6), and (3.8) contain terms proportional to a Dirac delta distribution of the form $f(\mathbf{x})\delta(\mathbf{x})$, where the function f can be singular at $\mathbf{x} = \mathbf{0}$. We replace these terms with $\mathrm{Pf}_0(f)\delta(\mathbf{x})$, where Pf_0 is the "Hadamard partie finie" of the function evaluated at its singular point $\mathbf{x} = \mathbf{0}$. The operation $\mathrm{Pf}_{\mathbf{x}_0}(f)$ for the function f which is singular at the point $\mathbf{x}_0$ is defined as follows: Let $\mathbf{n}$ be a unit vector; then one defines

$f_{\mathbf{n}}(\varepsilon) := f(\mathbf{x}_0 + \varepsilon \mathbf{n})$. One expands $f_{\mathbf{n}}$ into a Laurent series around $\varepsilon = 0$:

$$f_{\mathbf{n}}(\varepsilon) = \sum_{m=-N}^{\infty} a_m(\mathbf{n})\varepsilon^n.$$

The finite part of the function f is defined as the coefficient of ε^0 averaged over all directions:

$$\mathrm{Pf}_{\mathbf{x}_0}(f) := \frac{1}{4\pi} \oint d\Omega\, a_0(\mathbf{n}).$$

This way of regularizing singular functions was commonly used in numerous derivations of post-Newtonian equations of motion for point-particle systems (up to the fourth post-Newtonian order [14]), and it is best justified by dimensional regularization [15,16] (the limit $d \to 3$ of the d-dimensional version of the $\mathrm{Pf}_{\mathbf{x}_0}$ operation would give in our computations results identical with those obtained by means of the defined above three-dimensional version of this operation).

The solution of Eq. (3.8) can be written symbolically in the form

$$U_0(\mathbf{x}) = -\frac{GM_c}{|\mathbf{x}|} + U_0^D(\mathbf{x}), \qquad U_0^D(\mathbf{x}) := 4\pi G(\Delta^{-1}\rho_0)(\mathbf{x}).$$

$$(3.9)$$

Because $\mathrm{Pf}_{\mathbf{0}}(1/|\mathbf{x}|) = 0$, the term $U_0\delta(\mathbf{x})$ on the right-hand side of Eq. (3.8b) is replaced by $U_0^D(\mathbf{0})\delta(\mathbf{x})$, so the regularized form of this equation reads

$$\Delta U_1 = 4\pi G(M_c U_0^D(\mathbf{0})\delta(\mathbf{x}) + \rho_1 + 2p_0$$
$$+ \rho_0(h_0 - 2U_0 + 2r^2(v_0^\phi)^2)). \qquad (3.10)$$

The right-hand side of Eq. (3.5) contains $\partial_i U_0\delta(\mathbf{x})$, which is replaced by $\mathrm{Pf}_{\mathbf{0}}(\partial_i U_0)\delta(\mathbf{x})$. According to (3.9), one computes

$$\mathrm{Pf}_{\mathbf{0}}(\partial_i U_0) = \mathrm{Pf}_{\mathbf{0}}(GM_c x^i/|\mathbf{x}|^3 + \partial_i U_0^D(\mathbf{x}))$$
$$= 0 + \partial_i U_0^D(\mathbf{0}).$$

But $\partial_i U_0^D(\mathbf{0}) = 0$, because of the assumed axial and equatorial symmetry, and the whole term vanishes. Similarly, one can show that all terms with Dirac deltas in Eq. (3.6) vanish.

The Newtonian Euler equations (3.5) in cylindrical coordinates take the form

$$\partial_z h_0 = -\partial_z U_0, \qquad (3.11a)$$

$$\partial_r h_0 - r(v_0^\phi)^2 = -\partial_r U_0. \qquad (3.11b)$$

The 1PN Euler equations (3.6) written in cylindrical coordinates read

$$\partial_z h_1 = -\partial_z U_1 - v_0^\phi \partial_z A_\phi - (h_0 - 2U_0 - 2r^2(v_0^\phi)^2)\partial_z U_0$$
$$+ 2U_0\partial_z h_0, \qquad (3.12a)$$

$$\partial_r h_1 - 2rv_0^\phi v_1^\phi - r(v_0^\phi)^2(h_0 - 6U_0 + r^2(v_0^\phi)^2$$
$$= -\partial_r U_1 - v_0^\phi \partial_r A_\phi - (h_0 - 2U_0 - 2r^2(v_0^\phi)^2)\partial_r U_0$$
$$+ 2U_0\partial_r h_0. \qquad (3.12b)$$

One can use Newtonian equations (3.11) in order to simplify the 1PN equations (3.12). The result is

$$-\partial_z h_1 - \partial_z U_1 - v_0^\phi \partial_z A_\phi - (h_0 + 2r^2(v_0^\phi)^2)\partial_z U_0 = 0,$$
$$(3.13a)$$

$$-\partial_r h_1 - \partial_r U_1 + 2rv_0^\phi v_1^\phi - v_0^\phi \partial_r A_\phi + r^3(v_0^\phi)^4 + r(v_0^\phi)^2 h_0$$
$$- 4r(v_0^\phi)^2 U_0 - (h_0 + 2r^2(v_0^\phi)^2)\partial_r U_0 = 0. \qquad (3.13b)$$

It is easy to check, making use of $\partial_z v_0^\phi = 0$ (see the next section), that these two equations can be written as

$$\partial_z \Psi = 0, \qquad (3.14a)$$

$$\partial_r \Psi + 2rv_0^\phi v_1^\phi + A_\phi \partial_r v_0^\phi - 2r^2\partial_r(v_0^\phi)^2 h_0 = 0. \qquad (3.14b)$$

Here the function Ψ is defined as

$$\Psi = -h_1 - U_1 - v_0^\phi A_\phi + 2r^2(v_0^\phi)^2 h_0 - \frac{3}{2}h_0^2 - 4h_0 U_0$$
$$- 2U_0^2 - \int dr r^3(v_0^\phi)^4. \qquad (3.15)$$

The only nonzero vectorial component A_ϕ satisfies the following equation:

$$\Delta A_\phi - 2\frac{\partial_r A_\phi}{r} = -16\pi G r^2\rho_0 v_0^\phi. \qquad (3.16)$$

IV. THE INTEGRABILITY CONDITION

Differentiation of Eqs. (3.11a) and (3.11b)—the first one with respect to r and the second one with respect to z—and subtraction of the obtained equations leads to $\partial_z v_0^\phi = 0$. This is the consistency relation for the validity of the zeroth-order (Newtonian) approximation. That tells us that the Newtonian part of the rotation curve v_0^ϕ is an arbitrary function of the cylindrical radius r. It is well known that the requirement of stability imposes additional restrictions, through a growth condition imposed onto specific angular momentum in Newtonian and relativistic hydrodynamics [17–19].

The consistency condition for the 1PN approximation can be obtained from Eq. (3.14). Differentiating the first and second equations with respect to r and z, respectively, and subtracting the obtained equations, one arrives at

$$2rv_0^\phi \partial_z v_1^\phi + (\partial_r v_0^\phi)(\partial_z A_\phi) - 2r^2 \partial_r (v_0^\phi)^2 \partial_z h_0 = 0. \quad (4.1)$$

This constraint is resolved by

$$v_1^\phi = -\frac{A_\phi}{2rv_0^\phi} \partial_r v_0^\phi + \frac{rh_0}{v_0^\phi} \partial_r (v_0^\phi)^2, \quad (4.2)$$

as can be checked by direct inspection. We can summarize these results as follows:

Theorem. The 1PN equations (3.14) reduce to the algebraic equation

$$\Psi(r, z) = \text{const},$$

provided that the consistency condition

$$v_1^\phi = -\frac{A_\phi}{2rv_0^\phi} \partial_r v_0^\phi + 2rh_0 \partial_r v_0^\phi \quad (4.3)$$

is satisfied.

The interpretation of (4.3) is straightforward. The first term corresponds to the conventional frame dragging experienced by isolated test bodies in stationary spacetimes. The frame dragging is in this case a backreaction type effect—rotating disks generate (through Einstein equations) the metric function A_i, which in turn influences the rotation, via the first part of the formula (4.3). The other term is purely hydrodynamic, and it depends both on the rotation curve v_0^ϕ and on the specific enthalpy in the Newtonian approximation. It represents the direct 1PN reaction of rotating gas, proportional to the specific enthalpy, onto its own rotation.

Notice that A_ϕ and v_1^ϕ change sign when $v_0^\phi \to -v_0^\phi$; therefore, we consider only the case with $v_0^\phi \geq 0$.

V. SCALING SYMMETRY, NEWTONIAN ROTATION CURVES, AND 1PN APPROXIMATION

In what follows, we shall explain how the two terms in the expression of v_1^ϕ given in (4.3) influence rotation. It is easy to show that the dynamic part decelerates rotation. The specific enthalpy $h \geq 0$ is non-negative. Let us suppose a nonincreasing function $v_0^\phi(r)$, thence the term $v_{1\text{dyn}}^\phi := 2rh_0 \partial_r v_0^\phi$ is nonpositive—the instantaneous 1PN dynamic reaction slows the motion—"anti-drags" a system.

We prove that, in contrast to the above, the geometric dragging always increases the speed of rotation. The crucial part of the argument is to show, in the forthcoming lemma, that the function A_ϕ is non-negative. Taking this for granted and again assuming that $\partial_r v_0^\phi \leq 0$, we infer that $-\frac{A_\phi}{2rv_0^\phi} \partial_r v_0^\phi \geq 0$. Thus, a moving torus induces (via back-reaction) a geometry, that pushes the torus in the same direction; a rotating torus bootstraps itself.

Lemma. Assume that $\rho_0 \geq 0$, $v_0^\phi \geq 0$, both ρ_0 and v_0^ϕ are at least of Hölder class $C^{1,\mu}$, and that A_ϕ, the solution of (3.16), vanishes at infinity like $1/R$. Then A_ϕ is non-negative.

Proof. The potential A_ϕ vanishes at spatial infinity, and Eq. (3.16) with the conditions stated in the lemma above would satisfy assumptions of the minimum principle as stated in Refs. [20,21], save the term proportional to $1/r$, which is singular along the z-axis. Ignoring the latter, one would claim that from the minimum principle $A_\phi \geq 0$.

Due to the above difficulty, we shall adopt another approach to show that the solution is non-negative everywhere within the disk. We shall apply the method of contradiction. Let the solution of Eq. (3.16) exist on all of $\mathbf{R}^3$. Let there exist a region Ω that intersects the disk with $A_\phi \leq 0$ and that vanishes at an outer 2-surface S_∞ (S_∞ can be located at spatial infinity.) The potential A_ϕ is at least of class $C^{3,\mu}$, from the embedding theorems [20], and vanishes like $1/R$ at infinity. The complementary region (possibly empty) will be called Ω', and $A_\phi > 0$ on Ω'. The region Ω borders Ω' along a boundary $\partial\Omega$ with $A_\phi = 0$. The surface integrals $\int_{\partial\Omega} dS^i A_\phi \nabla_i A_\phi$ and $\int_{S_\infty} dS^i A_\phi \nabla_i A_\phi$ vanish, due to the boundary conditions.

Multiply Eq. (3.16) by A_ϕ over Ω and integrate by parts, This yields

$$-\int_\Omega dV (\nabla A_\phi)^2 = -16\pi G \int_\Omega dV r^2 \rho_0 v_0^\phi A_\phi. \quad (5.1)$$

The two boundary terms, that arise during integration by parts, vanish irrespective of whether Ω is bounded or unbounded. Since A_ϕ is differentiable and does not vanish identically, the left-hand side of (5.1) must be strictly negative. But if $A_\phi < 0$ in Ω, then the right-hand side is weakly positive. Thus, we get a contradiction: the solution A_ϕ cannot be negative within the disk volume.

Notice that the angular velocity of the fluid in the coordinate frame, $v^\phi = u^\phi/u^0$, is equal to the angular velocity of the fluid as seen by an observer at rest at infinity. The inverse of v^ϕ is proportional to the disk rotation period. Thus, the term v_1^ϕ is responsible for the 1PN correction to this period. Since the dynamic part $v_{1\text{dyn}}^\phi$ is decelerating rotation, it increases the rotation period. The drag term with A_ϕ in turn is positive, which means that it tends to shorten the rotation period.

One can find out that Newtonian and 1PN equations (3.8), (3.11), (3.12), and (3.16) are invariant under the following scalings:

$$\mathbf{x}' = \lambda \mathbf{x}, \quad M_c' = M_c, \quad \rho_0' = \frac{\rho_0}{\lambda^3}, \quad h_0' = \frac{h_0}{\lambda}, \quad v_0'^\phi = \frac{v_0^\phi}{\lambda^{3/2}},$$

$$U_0' = \frac{U_0}{\lambda}, \quad A_\phi' = \frac{A_\phi}{\sqrt{\lambda}}, \quad \rho_1' = \frac{\rho_1}{\lambda^4}, \quad h_1' = \frac{h_1}{\lambda^2},$$

$$v_1'^\phi = \frac{v_1^\phi}{\lambda^{5/2}}, \quad U_1' = \frac{U_1}{\lambda^2}. \quad (5.2)$$

These scalings imply that under this scaling operation,
  (1) the Newtonian disk mass as well as the total Newtonian mass are invariant.
  (2) the Newtonian pressure scales as $p_0' = p_0/\lambda^4$.

(3) the 1PN mass correction scales according to $M'_{1PN} = M_{1PN}/\lambda$.

The scaling of specific enthalpy entails the change of the equation of state. The coefficient K in the polytropic equation of state $p = K\rho^\gamma$ has to scale according to $K' = K\lambda^{3\gamma-4}$. If we assume the Keplerian rotation law (see Sec. VII), then the parameter $\omega'_0 = \omega_0$. The physical sense of this scaling is that the change of distances while keeping masses, associated with the appropriate adaptation of the equation of state and the rotation law, yields a new solution of the equations.

In our context, since the Newtonian Euler equations represent the zeroth-order approximation to the general-relativistic theory, we have to demand that the inner boundary of the disk be located outside of the Schwarzschild horizon, i.e., $(1 - U/c^2)r_{in} > 2GM_c/c^2$ [or even $(1 - U/c^2)r_{in} > 6GM_c/c^2$], while the speed of sound and the linear velocity rv_0^ϕ do not exceed the speed of light. These conditions limit our freedom in specifying the scaling parameter λ.

Equation (4.3) serves as the consistency condition; one easily finds that its right-hand side scales like $1/\lambda^{5/2}$, in agreement with the scaling of v_1^ϕ in (5.2). Collecting all these facts together, one immediately proves the following:

Conclusion. Let a solution of (3.11), 1PN equations (3.12), and Eq. (3.16) be obtained through rescalings specified in (5.2). Then its first post-Newtonian correction to the angular velocity scales as follows:

$$\frac{v_1'^\phi}{c^2 v_0'^\phi} = \frac{1}{\lambda} \frac{v_1^\phi}{c^2 v_0^\phi}.$$

Dust disks and uniformly rotating gas toroids are distinguished in a sense that becomes evident from the following description:

(i) *Uniform rotation.*—The correction term v_1^ϕ is proportional to the derivative of the angular velocity. Since for uniformly rotating systems $v_0^\phi = $ const, v_1^ϕ strictly vanishes. We conclude that in particular the rotation periods of rigidly rotating disks do not change in the 1PN perturbation order. That adds to the exceptional status of uniformly rotating disks, which are already known to minimize the total mass-energy for a given baryon number and total angular momentum [9,22].

(ii) *Dust.*—The pressure and specific enthalpy h_0 do vanish in the case of dust, which means that dust disks are exposed only to the frame dragging. The behavior of dust and gas disks are clearly different.

The rotation curve v_0^ϕ in the Newtonian approximation depends only on the distance from the rotation axis.

That means that even thick and self-gravitating Newtonian disks rotate uniformly along circles $z = $ const on cylinders of constant r. In contrast to that, the first post-Newtonian correction v_1^ϕ to the rotation curve is strictly determined by other quantities and depends on both r and z. The effective angular velocity is generically not constant along circles of constant height on cylinders with fixed values of the coordinate radius r and of the circumferential radius $(1 - U/c^2)r$.

VI. ON NUMERICAL METHOD

In the following, we will work in cylindrical (r, ϕ, z) or spherical (R, θ, ϕ) coordinates. For convenience, we will denote $\mu = \cos\theta$. We will also abuse the notation by reserving the same symbol for the given quantity in both coordinate systems.

We employ an iterative, self-consistent field (SCF)-type method based on solving two elliptic equations in axial symmetry: the standard scalar Poisson equation

$$\Delta\Phi = f(r, z) \tag{6.1}$$

and the vector equation of the form

$$\Delta\mathbf{A} = f(r, z)\mathbf{v}, \tag{6.2}$$

where in cylindrical (or spherical) coordinates the only nonvanishing components of fields $\mathbf{A}$ and $\mathbf{v}$ are $A_\phi d\phi$ and $v_\phi d\phi$, respectively. It is also assumed that $\partial_\phi A_\phi = \partial_\phi v_\phi = 0$. It is an easy exercise to check that A_ϕ satisfies

$$\Delta\left(\frac{\cos\phi A_\phi}{r}\right) = \frac{f(r, z)\cos\phi v_\phi}{r} \quad \text{or}$$
$$\Delta\left(\frac{\sin\phi A_\phi}{r}\right) = \frac{f(r, z)\sin\phi v_\phi}{r}. \tag{6.3}$$

This leads to the equation of the form

$$\Delta A_\phi - \frac{2\partial_r A_\phi}{r} = f(r, z)v_\phi.$$

These equations are solved by expanding the appropriate Green functions in Legendre functions. Although many drawbacks of such an approach are known, we prefer to follow it because of its conceptual simplicity. The following equations are known in the literature (in this or a similar form); we prefer to discuss them here for completeness.

The Green function of the flat three-dimensional Laplacian corresponding to a solution that vanishes asymptotically has the standard expansion

$$-\frac{1}{4\pi|\mathbf{x} - \mathbf{x}'|} = -\frac{1}{4\pi}\sum_{j=0}^\infty \frac{R_<^j}{R_>^{j+1}}\left\{P_j(\mu)P_j(\mu') + 2\sum_{m=1}^j \frac{(j-m)!}{(j+m)!}P_j^m(\mu)P_j^m(\mu')\cos[m(\phi - \phi')]\right\}, \tag{6.4}$$

where $R_{>(<)}$ denotes the larger (smaller) of the two radii R and R'. Using Eq. (6.4), one can write the solution of Eq. (6.1) as

$$\Phi(R,\mu) = -\frac{1}{2}\sum_{j=0}^{\infty} P_j(\mu)\left[\frac{1}{R^{j+1}}E_j(R) + R^j F_j(R)\right],\qquad(6.5)$$

where

$$E_j(R) = \int_0^R dR' R'^{j+2}\int_{-1}^1 d\mu' P_j(\mu')f(R',\mu')\qquad(6.6)$$

and

$$F_j(R) = \int_R^\infty dR' \frac{1}{R'^{j-1}}\int_{-1}^1 d\mu' P_j(\mu')f(R',\mu').\qquad(6.7)$$

Note that if $f(R,\mu)$ is equatorially symmetric (i.e., it is an even function of μ), integrals with $P_{2j+1}(\mu)$ vanish. In this case it is also enough to integrate with respect to μ over $0 \le \mu \le 1$. The numerical implementation of the above formulas is straightforward; it is discussed, for instance, in Ref. [23].

Equation (6.2) can be solved in a similar fashion, which is equivalent to finding of a suitable expansion of the Green function for the operator $\Delta - (2/r)\partial_r$. One can start with Eq. (6.3). Using Eq. (6.4), the solution for $\cos\phi A_\phi/(R\sqrt{1-\mu^2})$ can be written as

$$\frac{\cos\phi A_\phi(R,\mu)}{R\sqrt{1-\mu^2}} = -\frac{1}{4\pi}\int_0^\infty dR' R' \int_{-1}^1 \frac{d\mu'}{\sqrt{1-\mu'^2}}\int_0^{2\pi} d\phi' \cos\phi' f(R',\mu')v_\phi(R',\mu')$$
$$\times \sum_{j=0}^\infty \frac{R_<^j}{R_>^{j+1}}\left\{P_j(\mu)P_j(\mu') + 2\sum_{m=1}^j \frac{(j-m)!}{(j+m)!}P_j^m(\mu)P_j^m(\mu')\cos[m(\phi-\phi')]\right\}.$$

The integral

$$I = \int_0^{2\pi} d\phi' \cos\phi' \cos[m(\phi-\phi')]$$

can be easily evaluated. For $m = 1$, one has $I = \pi\cos\phi$. For $m \ne 1$, one has

$$I = \frac{2m\sin(m\pi)\cos[m(\pi-\phi)]}{(m-1)(m+1)}.$$

This yields

$$\frac{\cos\phi A_\phi(R,\mu)}{R\sqrt{1-\mu^2}} = -\frac{1}{2}\cos\phi\int_0^\infty dR' R' \int_{-1}^1 \frac{d\mu'}{\sqrt{1-\mu'^2}}f(R',\mu')v_\phi(R',\mu')\sum_{j=1}^\infty \frac{R_<^j}{R_>^{j+1}}\frac{1}{j(j+1)}P_j^1(\mu)P_j^1(\mu').$$

And finally,

$$A_\phi(R,\mu) = -\frac{1}{2}\sqrt{1-\mu^2}\sum_{j=1}^\infty \frac{1}{j(j+1)}P_j^1(\mu)\left[\frac{1}{R^j}C_j(R) + R^{j+1}D_j(R)\right],\qquad(6.8)$$

where

$$C_j(R) = \int_0^R dR' R'^{j+1}\int_{-1}^1 \frac{d\mu'}{\sqrt{1-\mu'^2}}P_j^1(\mu')f(R',\mu')v_\phi(R',\mu')\qquad(6.9)$$

and

$$D_j(R) = \int_R^\infty dR' \frac{1}{R'^j}\int_{-1}^1 \frac{d\mu'}{\sqrt{1-\mu'^2}}P_j^1(\mu')f(R',\mu')v_\phi(R',\mu').\qquad(6.10)$$

Of course, $d\mu/\sqrt{1-\mu^2} = -d\theta$. Note that

$$P_{2j}^1(\mu) = \sqrt{1-\mu^2}\,\frac{d}{d\mu}P_{2j}(\mu)$$

(where we use the convention without Condon-Shortley's phase). The derivatives $dP_{2j}(\mu)/d\mu$ are odd functions of μ, and $f(R,\mu)v_\phi(R,\mu)$ are symmetric under reflection $z \to -z$. Therefore, all integrals with P_{2j}^1 vanish.

Note also that Eq. (6.3) is equivalent to the equation

$$\Delta f + \frac{2}{R}\partial_R f - \frac{2}{R^2}\mu\partial_\mu f = S(R,\mu)$$

that appears in Refs. [11,12,24,25]. In cylindrical coordinates, the above equation can be rewritten as

$$\partial_r^2 f + \partial_z^2 f + \frac{3}{r}\partial_r f = S(r,z).$$

Setting $\psi = r\cos\phi f$, it is easy to show that ψ satisfies

$$\Delta_{(r,z,\phi)}\psi = r\cos\phi\left(\partial_r^2 f + \partial_z^2 f + \frac{3}{r}\partial_r f\right)$$

$$= r\cos\phi S(r,z).$$

In the description of the numerical method given below, we specialize to the Keplerian rotation law $v_0^\phi = \omega_0/r^{3/2}$ and polytropic equations of state $p_0 = K\rho_0^{5/3}$.

The method of obtaining the solutions of the zeroth-order approximation (Newtonian solutions) was described in detail in Ref. [3]. Equations to be solved are

$$\Delta U_0^{\mathrm{D}} = 4\pi G\rho_0 \tag{6.11}$$

and

$$h_0 + \Phi_c - \frac{GM_c}{R} + U_0^{\mathrm{D}} = C, \tag{6.12}$$

where the centrifugal potential is given by

$$\Phi_c = -\int^r dr' r'(v_0^\phi(r'))^2 = \frac{\omega_0^2}{r}, \tag{6.13}$$

and the specific enthalpy reads $h_0 = 5K\rho_0^{2/3}/2$. These equations are solved iteratively: in each iteration step one obtains a solution for U_0^{D} based on the previous density distribution. A new distribution of the enthalpy h_0 (or, equivalently, ρ_0) is then computed from Eq. (6.13). Also, in each iteration step we renormalize the constants C and K, so that the resulting disk has the prescribed values of the inner and outer radii and the maximum density. We use a spherical numerical grid. The solution of Eq. (6.11) is computed by truncating expansion (6.5) at a sufficiently

large number of Legendre polynomials. Integrals (6.6) and (6.7) are computed using standard quadrature formulas.

The 1PN corrections are obtained by solving equations

$$\Delta A_\phi - \frac{2\partial_r A_\phi}{r} = -16\pi G\omega_0\sqrt{r}\rho_0, \tag{6.14}$$

$$\Delta U_1 = 4\pi G(M_c U_0^{\mathrm{D}}(\mathbf{0})\delta(\mathbf{x}) + \rho_1 + 2K\rho_0^{5/3}$$
$$+ \rho_0(h_0 - 2U_0 + 2\omega_0^2 r^{-1})), \tag{6.15}$$

$$h_1 = -U_1 - A_\phi\omega_0 r^{-3/2} + 2h_0\omega_0^2 r^{-1} + \frac{1}{2}\omega_0^4 r^{-2}$$
$$- \frac{3}{2}h_0 - 4h_0 U_0 - 2U_0^2 - C_1 \tag{6.16}$$

for A_ϕ, U_1, h_1 and ρ_1. Here the Newtonian gravitational potential is given by $U_0 = -GM_c/R + U_0^{\mathrm{D}}$. The 1PN corrections to the density ρ_1 and the enthalpy h_1 are related by $h_1 = 5K\gamma\rho_0^{2/3}\rho_1/3$.

Once the zeroth-order approximation is known, the potential A_ϕ can be obtained from Eq. (6.14) using the expansion given by Eq. (6.8). In the next step we iterate Eqs. (6.15) and (6.16) in a similar way to that used to obtain the zeroth-order solution.

The term $4\pi GM_c U_0(\mathbf{0})\delta(x)$ on the right-hand side of Eq. (6.16) yields the term $-GM_c U_0^{\mathrm{D}}(\mathbf{0})/R$ in the solution for U_1. Note that, although it is convenient to exclude the origin $\mathbf{x} = \mathbf{0}$ from the numerical grid, the value $U_0^{\mathrm{D}}(\mathbf{0})$ can still be easily computed as

$$U_0^{\mathrm{D}}(\mathbf{0}) = -G\int d^3x\frac{\rho_0}{R}.$$

In each of the iterations of the Newtonian scheme, the value of the enthalpy is obtained from Eq. (6.12). We set $\rho_0 = h_0 = 0$ whenever this equation yields a negative value of h_0. This is the key element of our implementation of the free-boundary SCF-type scheme, that allows us to compute the true boundary of the disk. Similarly, in the post-Newtonian scheme, we obtain the value of h_1 from Eq. (6.16). We set $h_1 = \rho_1 = 0$, whenever $h_0 + h_1/c^2 \le 0$ or $\rho_0 + \rho_1/c^2 \le 0$.

The constant C_1 appearing in Eq. (6.16) is renormalized so that in each iteration the correction h_1 to the enthalpy vanishes at the outer end of the Newtonian disk, in the plane $z = 0$. In this way a full post-Newtonian solution is obtained for a specified value of the outer radius.

VII. DISCUSSION OF NUMERICAL RESULTS

We report in this section numerical results on modeling black hole–disk systems. Disks' masses are taken in the range $1–2 \times M_c$, where M_c is the mass of the central black hole. The Keplerian rotation law and the polytropic equation of state are assumed, as in the preceding section.
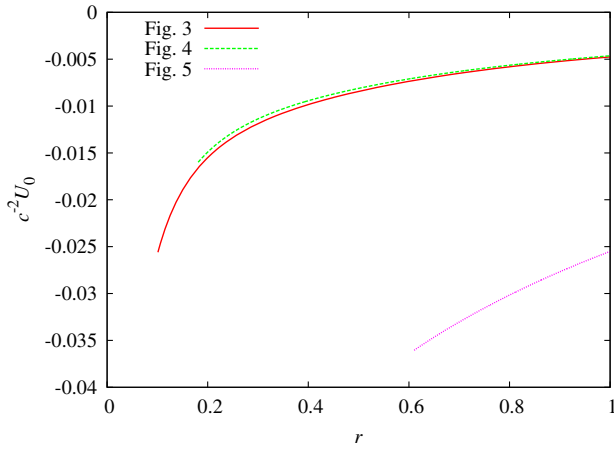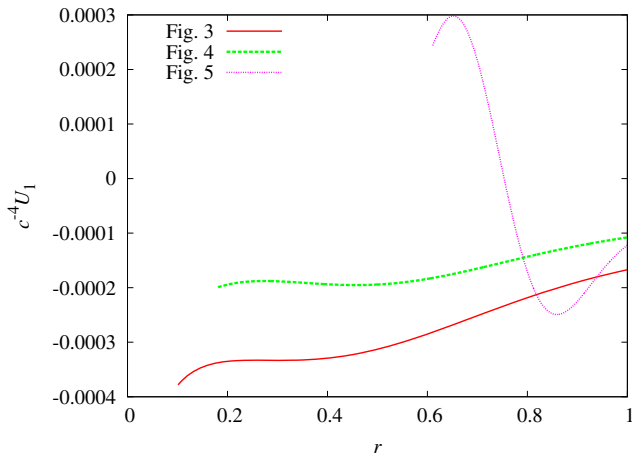
FIG. 1 (color online). The ordinate shows the value of U_0/c^2 along the ray $\phi = \text{const}$ on the central plane $z = 0$ and the abscissa the normalized coordinate distance r/r_{out} from the center. The dotted line corresponds to the solution described in Fig. 5, while the broken and solid lines refer to solutions described in Figs. 4 and 3, respectively.

We carefully choose parameters in all forthcoming examples so that the 1PN approximation can be valid. The largest linear velocities $(1 - U)rv^{\phi}$ at the inner part of the disks are of the order of one tenth the speed of light. The graphs of the normalized Newtonian and 1PN potentials, U_0/c^2 and U_1/c^4, respectively, are displayed in Figs. 1 and 2. It is clear from Fig. 1 that $1 \gg |U_0|/c^2$. The comparison of Figs. 1 and 2 implies that the 1PN correction $|U_1|/c^4$ constitutes about one hundredth of the main Newtonian contribution.

The black and white shaded palettes in Figs. 3–5 describe the ratio $v_1^{\phi}/(c^2 v_0^{\phi})$ within the disk volume. In

FIG. 2 (color online). The ordinate shows the value of U_1/c^2 along the ray $\phi = \text{const}$ on the central plane $z = 0$ and the abscissa the normalized coordinate distance r/r_{out} from the center. The dotted line corresponds to the solution described in Fig. 5, while the broken and solid lines refer to solutions described in Figs. 4 and 3, respectively.
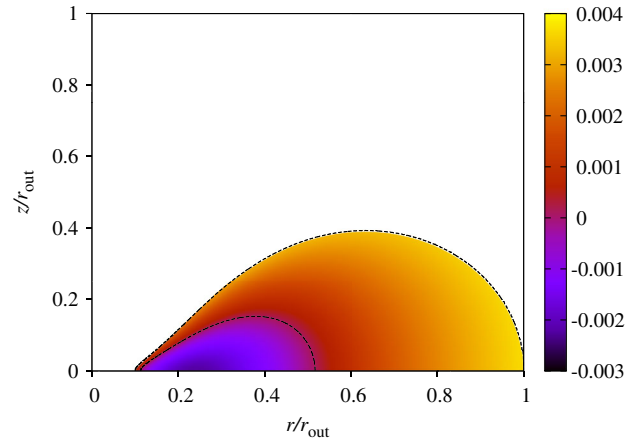

FIG. 3 (color online). The ratio $v_1^{\phi}/(c^2 v_0^{\phi})$ within the disk volume. The ordinate shows the height of the disk and the abscissa the coordinate distance from the center, in the rescaled unit system r/r_{out} where $r_{\text{out}} \equiv 250 R_{\text{S}}$. The inner disk boundary is located at $r_{\text{in}} = 25 R_{\text{S}}$, and the outer boundary at $r_{\text{out}} = 250 R_{\text{S}}$. The Newtonian disk mass $M_{\text{D}} = 1.47 \times M_{\text{c}}$. The white region is dominated by dynamic braking; its boundary is denoted by the short broken line, where the 1PN velocity correction v_1^{ϕ} vanishes. The drag is strongest at the disk boundary. Here $\omega_0 = 0.85\sqrt{2GM_{\text{c}}}$.

all examples, $R_{\text{S}} := 2GM_{\text{c}}/c^2$ is the Schwarzschild radius of the central black hole.

Keplerian disks are influenced by both the geometric dragging and the anti-dragging dynamic effects. In Fig. 3, one sees an inner zone shifted to the center with the prevailing braking component (the Newtonian angular velocity v_0^{ϕ} is diminished by the 1PN correction up to 0.3%), and the outer part where the drag component dominates (the Newtonian angular velocity v_0^{ϕ} is enhanced by up to 0.4%). The innermost part of the disk is at the coordinate distance $r_{\text{in}} = 25 R_{\text{S}}$ from the central black hole, while the outermost disk boundary is at $r_{\text{out}} = 250 R_{\text{S}}$. Notice that the circumferential radius $(1 - U/c^2)r + \mathcal{O}(c^{-4})$ is well approximated by the coordinate r due to the smallness of potentials.

Our numerical investigation suggests that one can find an infinite number of similar configurations simply by moving out the inner disk positions up to 18% of the coordinate size. Somewhere between the rescaled inner boundary position 0.18 and 0.19 the character of the picture changes—the anti-dragging nowhere dominates, and all parts of disks are dragged forward. This limiting-type configuration is shown in Fig. 4. It remains to be explained in what circumstances the dynamic effect can overcome the geometric dragging. Our empirical observation is that if the relative width $w := (r_{\text{out}} - r_{\text{in}})/r_{\text{out}} > 0.2$, then the latter effect is stronger, and the smaller the w, the smaller the dynamic braking.

We found in a number of examples that the maximal value of the ratio of the 1PN corrections to the Newtonian angular velocities $v_1^{\phi}/(c^2 v_0^{\phi})$ can achieve a few percent.
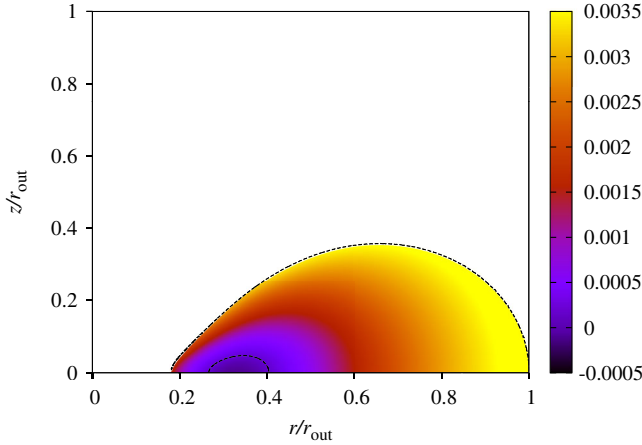
FIG. 4 (color online). The ratio $v_1^\phi/(c^2 v_0^\phi)$ within the disk volume for the limiting-type system. The ordinate shows the height of the disk and the abscissa the coordinate distance from the center, in the rescaled unit system $r/r_{\rm out}$ where $r_{\rm out} \equiv 450 R_{\rm S}$. The inner disk boundary is located at $r_{\rm in} = 81 R_{\rm S}$, and the outer boundary at $r_{\rm out} = 450 R_{\rm S}$. The Newtonian disk mass $M_{\rm D} = 1.4 \times M_{\rm c}$. The white region is dominated by dynamic braking; its boundary is denoted by the short broken line, where the 1PN velocity correction v_1^ϕ vanishes. The drag is strongest at the disk boundary. Here $\omega_0 = 1.188 \sqrt{2 G M_{\rm c}}$.

Figure 5 describes a strongly relativistic compact system, with the disk width smaller than $19.5 R_{\rm S}$ and relatively large 1PN effects. The dynamic anti-dragging effect manifests here only by a slight diminishing of the ratio $v_1^\phi/(c^2 v_0^\phi)$ within the inner part of the central zone.

We already pointed out in Sec. V that one can rescale a given solution within the 1PN approximation according to the recipe defined in (5.2). Physical distances do change
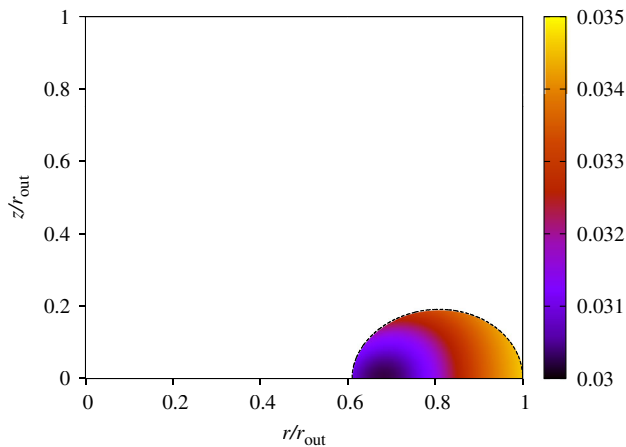

FIG. 5 (color online). The ratio $v_1^\phi/(c^2 v_0^\phi)$ within the disk volume. The ordinate shows the height of the disk and the abscissa the coordinate distance from the center, in the rescaled unit system $r/r_{\rm out}$ where $r_{\rm out} = 50 R_{\rm S}$. The inner boundary is located at $r_{\rm in} = 30.5 R_{\rm S}$, and the outer boundary at $r_{\rm out} = 50 R_{\rm S}$. The disk mass $M_{\rm D} = 1.8 \times M_{\rm c}$. The drag is strongest at the disk boundary, up to 3.46%. Here $\omega_0 = 1.31 \sqrt{2 G M_{\rm c}}$.

under rescalings, but the central mass and the disk mass are invariant. At the same time, the relative velocity correction scales as $v_1'^\phi/v_0'^\phi \propto 1/\lambda$; thus, in principle one can generate from a given solution a sequence of configurations with identical masses, different geometrical distances, and with a different ratio $v_1^\phi/(c^2 v_0^\phi)$. One can do that with any of the three already depicted disk configurations. That suggests, in particular, that one can generate disk systems with a very large 1PN correction to the angular velocity. There is, however, a question whether these rescaled solutions can be regarded as being tangent to the solution of the exact general-relativistic hydrodynamics. The answer to that cannot be found in the 1PN analysis, but must be sought with the exact general-relativistic treatment. We leave this problem for future investigation.

VIII. SUMMARY

We investigated stationary gaseous disks around a spinless black hole in the 1PN approximation scheme. The 1PN calculation is obviously simpler technically than the full general-relativistic picture, but it does include essential features—the nonlinearity and backreaction—that are typical for Einstein equations. The concepts of the quasilocal masses and angular momentum can be meaningfully defined in stationary axially symmetric systems, but it is useful that the 1PN approximation is based on Newtonian concepts and Newtonian intuition. The 1PN approximation allows for flexibility in imposing rotation laws that correspond to well-known classes of Newtonian rotation curves, including the Keplerian rotation. We took care to deal with relatively small characteristic velocities and potentials, $v/c \ll 1$ and $|U|/c^2 \ll 1$, in all calculations reported here; that should guarantee that 1PN results are correct. The main results are as follows:

An integrability condition leads to the emergence of two distinctly different types of general-relativistic corrections to the angular velocity.

One of them is due to the familiar geometric dragging of frames; this depends *only indirectly* on the disk structure and rotation, because the metric in the 1PN expansion does include the backreaction and indirectly depends on characteristics of matter at the Newtonian level. The other type—the dynamic effect—that directly depends on the material structure of a disk, has been hitherto unknown. That one is strongest in the central disk plane.

The geometric and dynamic effects counteract; the dragging of frames pushes a disk forward, but the dynamic effect diminishes the angular velocity. In many numerical solutions, the net effect had been weakest in a central zone of the disk. Inside of that zone, the gas may be actually slowed down (the total 1PN angular velocity correction may or can be negative), while at its boundary the dynamic correction vanishes. The geometric dragging of frames always dominates in the disk boundary zone.

The 1PN correction to the orbital period can be significant. We found a number of numerical models that satisfy requirements of the 1PN approximation—with a change of the orbital period close to 4%. The Newtonian and 1PN equations posses a scaling symmetry that in principle would generate new solutions with even larger 1PN corrections to the angular velocity. These rescaled solutions have to satisfy the assumptions of the 1PN approximations. The ultimate answer concerning whether or not they approximate exact solutions would require the investigation of an exact general-relativistic model.

We found that there is one type of matter—dust—for which the dynamic effect vanishes. Disks made of dust experience 1PN corrections only through the dragging of frames. It is interesting that uniformly rotating disks do not show any 1PN effect—both contributory effects, the geometric dragging of frames and the dynamic one, do vanish in this case.

In the merger of compact binaries consisting of pairs of black holes and neutron stars, a neutron star is destroyed [26] and a heavy leftover disk would form, that might reveal signs of the anti-dragging. The Bardeen-Petterson effect [27], that arises due to the geometric dragging, is known to occur in some AGNs [28]. The dynamic braking may lead to its observable modifications in black hole–(heavy) disk systems.

[1] J. E. Pringle, Annu. Rev. Astron. Astrophys. **19**, 137 (1981).

[2] I. D. Novikov and K. S. Thorne, in *Black Holes (Les Astres Occlus)*, edited by C. DeWitt and B. S. DeWitt (Gordon and Breach, New York, 1973), pp. 343–450.

[3] P. Mach, E. Malec, and M. Piróg, Acta Phys. Pol. B **44**, 107 (2013).

[4] P. Mach, E. Malec, and M. Piróg, Acta Phys. Pol. B **43**, 2141 (2012).

[5] L. Blanchet, T. Damour, and G. Schäfer, Mon. Not. R. Astron. Soc. **242**, 289 (1990).

[6] J. M. Bardeen and R. A. Wagoner, Astrophys. J. **158**, L65 (1969).

[7] V. Karas, J.-M. Huré, and O. Semerák, Classical Quantum Gravity **21**, R1 (2004).

[8] M. Abramowicz and P. Fragile, Living Rev. Relativity **16**, 1 (2013).

[9] N. Stergioulas, Living Rev. Relativity **6**, 3 (2003).

[10] L. G. Fishbone and V. Moncrief, Astrophys. J. **207**, 962 (1976).

[11] S. Nishida and Y. Eriguchi, Astrophys. J. **427**, 429 (1994).

[12] S. Nishida, Y. Eriguchi, and A. Lanza, Astrophys. J. **401**, 618 (1992).

[13] M. Ansorg and D. Petroff, Phys. Rev. D **72**, 024019 (2005).

[14] P. Jaranowski and G. Schäfer, Phys. Rev. D **87**, 081503(R) (2013).

[15] T. Damour, P. Jaranowski, and G. Schäfer, Phys. Lett. B **513**, 147 (2001).

[16] L. Blanchet, T. Damour, and G. Esposito-Farèse, Phys. Rev. D **69**, 124007 (2004).

[17] J.-L. Tassoul, *Stellar Rotation* (Cambridge University Press, Cambridge, UK, 2007).

[18] F. H. Seguin, Astrophys. J. **197**, 745 (1975).

[19] J. L. Friedman and N. Stergioulas, Bull Astron Soc India **39**, 21 (2011).

[20] L. C. Evans, *Partial Differential Equations* (American Mathematical Society, Providence, RI, 1998).

[21] D. Gilbarg and N. Trudinger, *Elliptic Partial Differential Equations of Second Order* (Springer, New York, 1983).

[22] R. H. Boyer and R. W. Lindquist, Phys. Lett. **20**, 504 (1966).

[23] E. Müller and M. Steinmetz, Comput. Phys. Commun. **89**, 45 (1995).

[24] H. Komatsu, Y. Eriguchi, and I. Hachisu, Mon. Not. R. Astron. Soc. **237**, 355 (1989).

[25] S. Bonazzola and J. Schneider, Astrophys. J. **191**, 273 (1974).

[26] F. Pannarale, A. Tonita, and L. Rezzolla, Astrophys. J. **727**, 95 (2011).

[27] J. Bardeen and J. Petterson, Astrophys. J. **195**, L65 (1975).

[28] J. Moran, ASP Conf. Ser. **395**, 87 (2008).